

Bit-Interleaved Polar-Coded OFDM for Low-Latency M2M Wireless Communications

Koike-Akino, T.; Wang, Y.; Draper, S.C.; Sugihara, K.; Matsumoto, W.

TR2017-042 May 2017

Abstract

Machine-to-machine (M2M) communications play an important role for applications that involve connections between a massive number of heterogeneous devices in home and industrial networks. For M2M networks, realizing low latency and high reliability is of great importance. In this paper, we show the great potential of polar-coded orthogonal frequency-division multiplexing (OFDM) to fulfill those requirements. We show that polar codes with list decoding plus cyclic redundancy check (CRC) can outperform state-of-the-art low-density parity-check (LDPC) codes at short block lengths. In addition, we introduce an efficient interleaver and constellation shaping for polar-coded high-order modulations, where a coded sequence is carefully mapped across subcarriers and modulation bits to exploit nonuniform reliability for higher diversity gains. Through computer simulations, we demonstrate that a significant gain greater than 2 dB can be achieved by quadratic polynomial permutation (QPP) interleaver with optimized parameters in comparison to the conventional random interleaver for high-order 256-ary quadrature-amplitude modulation (QAM) OFDM transmission in frequency-selective wireless channels.

IEEE International Conference on Communications (ICC)

This work may not be copied or reproduced in whole or in part for any commercial purpose. Permission to copy in whole or in part without payment of fee is granted for nonprofit educational and research purposes provided that all such whole or partial copies include the following: a notice that such copying is by permission of Mitsubishi Electric Research Laboratories, Inc.; an acknowledgment of the authors and individual contributions to the work; and all applicable portions of the copyright notice. Copying, reproduction, or republishing for any other purpose shall require a license with payment of fee to Mitsubishi Electric Research Laboratories, Inc. All rights reserved.

Bit-Interleaved Polar-Coded OFDM for Low-Latency M2M Wireless Communications

Toshiaki Koike-Akino*, Ye Wang*, Stark C. Draper†, Kenya Sugihara‡, Wataru Matsumoto‡

*Mitsubishi Electric Research Laboratories (MERL), 201 Broadway, Cambridge, MA 02139, USA

†Electrical & Computer Engineering, University of Toronto, Toronto, ON M5S 3G4, Canada

‡Information Technology R&D Center, Mitsubishi Electric Corporation, 5-1-1 Ohuna, Kanagawa, 247-8501 Japan

Email: {koike, yewang}@merl.com, stark.draper@utoronto.ca, sugihara.kenya@dx.mitsubishielectric.co.jp

Abstract—Machine-to-machine (M2M) communications play an important role for applications that involve connections between a massive number of heterogeneous devices in home and industrial networks. For M2M networks, realizing low latency and high reliability is of great importance. In this paper, we show the great potential of polar-coded orthogonal frequency-division multiplexing (OFDM) to fulfill those requirements. We show that polar codes with list decoding plus cyclic redundancy check (CRC) can outperform state-of-the-art low-density parity-check (LDPC) codes at short block lengths. In addition, we introduce an efficient interleaver and constellation shaping for polar-coded high-order modulations, where a coded sequence is carefully mapped across subcarriers and modulation bits to exploit non-uniform reliability for higher diversity gains. Through computer simulations, we demonstrate that a significant gain greater than 2 dB can be achieved by quadratic polynomial permutation (QPP) interleaver with optimized parameters in comparison to the conventional random interleaver for high-order 256-ary quadrature-amplitude modulation (QAM) OFDM transmission in frequency-selective wireless channels.

I. INTRODUCTION

Machine-to-machine (M2M) communications systems enable machines to exchange short command and control messages over wireless links. One of the major applications of M2M communications includes industrial factory network, wherein automated production processes can benefit from wireless communications between machines. Such applications call for both low latency and high reliability in the transmission of short messages over wireless networks [1], and in practice it is often preferable to equip only one antenna for small, simple, and cost/power-efficient devices.

In order to achieve low latency, short block lengths, e.g., less than a few hundreds of symbols, may be required. However, with such short block lengths, it is difficult to fulfill the high reliability requirement, since we cannot rely on capacity-achieving forward error correction (FEC) codes such as low-density parity-check (LDPC) codes [2–6], which would typically require lengths longer than 10000 bits to approach capacity. Besides the issue of short-length FEC bound [7], we have another challenge in exploiting time diversity to deal with wireless channel fading for short-message communications. In addition, single-antenna systems cannot use spatial diversity techniques [8–11] as well as time diversity.

In the absence of diversity availability in space and time domain, frequency diversity is the most promising alternative

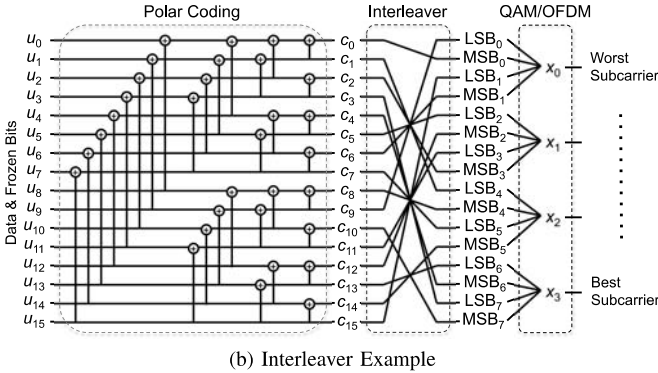
to consider for reliable wireless communications in M2M fading channels. In order to achieve higher frequency diversity gain in M2M channels, precoding methods [11–15] have been investigated. For example, random phase precoding with discrete Walsh–Hadamard transform instead of discrete Fourier transform (DFT) can achieve near exponential diversity order by means of shuffling and mixing signal constellations before transmission. However, such precoding methods require complicated equalization techniques such as probabilistic data association (PDA) [14, 15]. In consequence, orthogonal frequency-division multiplexing (OFDM) based on DFT has still been used in general to cope with inter-symbol interference by one-tap equalization in frequency-selective fading channels. For such OFDM transmission systems, we usually need FEC codes distributed across different subcarriers to achieve frequency diversity.

In this paper, we investigate polar codes [16–23] as strong candidates for M2M wireless communications using short-block OFDM transmission to achieve high diversity and coding gains. Polar codes have drawn significant attention in the coding theory community since Arıkan proved in 2009 [16] that polar codes achieve capacity over any arbitrary discrete-input memoryless channels when paired with low-complexity successive-cancellation (SC) decoding. However, in spite of their theoretical strength, polar codes have not yet been adopted in practical systems due to their poor performance at short block lengths in comparison to LDPC codes. A major breakthrough was made in 2015 when Tal and Vardy [18] introduced list decoding and an embedded cyclic redundancy check (CRC) to make polar codes competitive with LDPC codes. It was also shown in [19] that the polar coding with list+CRC decoding can approach Polyanskiy’s finite-length capacity bound [7], at short block lengths suited for M2M communications.

We extend the work of bit-interleaved polar-coded modulation [23, 24] to M2M wireless fading channels. It was shown in [23, 24] that careful mapping of coded bits to modulation bits offers approximately 0.5 dB gain over the conventional random interleaving for high-order quadrature-amplitude modulation (QAM) in additive white Gaussian noise (AWGN) channels. We further improve the performance by designing interleaver for polar-coded OFDM transmission in fading channels, so that higher frequency diversity gain can



(a) Transmission Flowchart



(b) Interleaver Example

Fig. 1. Bit-interleaved polar-coded modulation. Frozen bit and interleaving are designed for high-order modulation and OFDM transmission, where different subcarriers and modulation bits have non-identical reliability to exploit diversity.

be achieved within a single OFDM symbol for low-latency M2M wireless networks. We also discuss non-uniform QAM constellations to achieve additional shaping gain [25–27] for polar-coded systems. In comparison to existing works, the main contributions of this paper are summarized below.

- **One-Shot Polar-Coded OFDM:** In order to minimize the latency for M2M applications, we consider the use of short block-length polar coding mapped onto only a single OFDM symbol.
- **Adaptive Interleaving:** We show that well-designed interleaving that is adaptive to channel selectivity can achieve a greater-than 2 dB diversity gain compared to random interleaving for polar-coded OFDM transmission.
- **Non-uniform QAM Shaping:** We introduce a deterministic constellation shaping based on a super-Gaussian distribution for high-order QAM signaling to improve the performance of polar-coded OFDM.

II. M2M WIRELESS COMMUNICATIONS SYSTEM

A. System Description

We consider M2M communications from a transmitter to a receiver, each of which is equipped with a single antenna, over wireless fading channels. Fig. 1 shows a schematic of the M2M communications system, which uses polar-coded OFDM transmission over wireless M2M channels. The OFDM transmission has been widely used in wireless communications as no complicated equalization techniques are required to combat inter-symbol interference in frequency-selective fading channels. The transmitter uses a single OFDM symbol to send an N -bit codeword block, $\mathbf{c} = [c_0, c_1, \dots, c_{N-1}]^T$, where $c_n \in \mathbb{Z}_2$ is the n th coded bit (\mathbb{Z}_q is a non-negative integer set less than q) and the superscript $[\cdot]^T$ denotes a transpose. The codeword is interleaved and modulated by M^2 -ary QAM

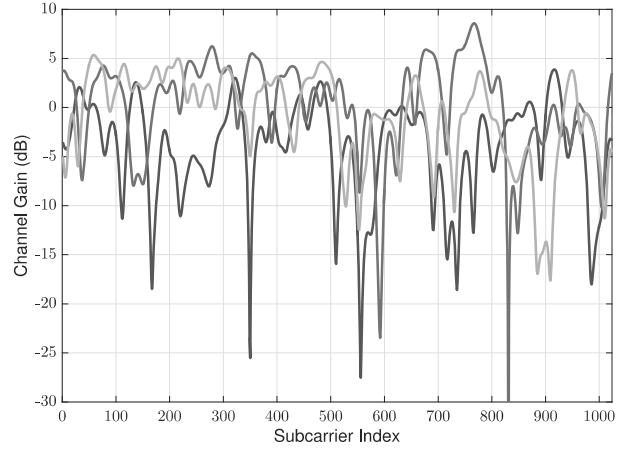


Fig. 2. Example realizations of selective channel gains for OFDM transmission ($N' = 1024$) over Nakagami–Rice fading channels ($K = 0$ dB) with exponentially decaying delay profile (0.5 dB decay per symbol delay).

(M is assumed a power-of-two integer), followed by OFDM signaling. Let $\mathbf{x} = [x_0, x_1, \dots, x_{N'}]^T$ be the QAM-modulated symbols, where $N' = N/\log_2(M^2)$ is the total number of subcarriers in use. We assume that the energy of modulated signals is normalized as $\mathbb{E}[|x_n|^2] = 1$, where $\mathbb{E}[\cdot]$ denotes expectation. To realize minimum possible latency, we consider the use of short-length polar coding, whose codeword block is mapped within only one OFDM symbol.

Here, we assume a cyclic prefix (CP) to prevent inter-block interference. Through wireless fading channels, the receiver obtains the received signal block $\mathbf{y} = [y_0, y_1, \dots, y_{N'-1}]^T \in \mathbb{C}^{N' \times 1}$, which is modeled after CP removal as follows:

$$\mathbf{y} = \mathbf{h} \circ \mathbf{x} + \mathbf{z}, \quad (1)$$

where $\mathbf{h} \in \mathbb{C}^{N' \times 1}$ is a channel coefficient vector in frequency domain, \circ denotes Hadamard product, and $\mathbf{z} = [z_0, z_1, \dots, z_{N'-1}]^T \in \mathbb{C}^{N' \times 1}$ is an additive noise vector. The noise vector \mathbf{z} comes from a zero-mean circular-symmetric complex Gaussian distribution of $\mathcal{CN}(\mathbf{0}, \sigma^2 \mathbf{I}_{N'})$ having a covariance matrix of $\sigma^2 \mathbf{I}_{N'}$, where $\mathbf{I}_{N'}$ is an identity matrix of size $N' \times N'$. After QAM demodulation, the receiver provides log-likelihood data to feed into the polar decoder, which employs list+CRC decoding.

B. M2M Wireless Fading Channels

It is known that wireless channels are well modeled by Nakagami–Rice fading or log-normal fading in industrial M2M environment [1]. Fig. 2 illustrates three examples of channel realizations for Nakagami–Rice fading with a Rice factor of $K = 0$ dB. Here, we assume an exponentially decaying delay profile, whose decay factor is 0.5 dB per sample delay. We observe that the channel gain can deeply fade by tens of dB across selective subcarriers even for the line-of-sight (LOS) condition. In general, such frequency-selective fading can induce a significant penalty, whereas the polar-coded OFDM mapped across subcarriers can exploit diversity to mitigate the loss for single-antenna latency-constrained

systems (i.e., lack in diversity availability over space and time domain but frequency).

C. Motivations

In this paper, we design an interleaver for polar coding to improve the diversity gain. In [23, 24], it was shown that careful design of interleaving can provide approximately 0.5 dB gain in AWGN channels, by boosting the polarization phenomenon of polar coding through effective mapping of coded bits onto QAM symbols, which have non-identical reliability across most- to least-significant bits (MSB/LSB). We extend the work to OFDM signaling for wireless M2M channels, in which there is more significant non-uniformity in bit likelihoods due to frequency-selective fading as shown in Fig. 2. We later demonstrate that a well-designed interleaver can achieve a significant diversity gain that is greater than 2 dB in comparison to conventional random and block interleavers in wireless channels.

III. POLAR CODES WITH LIST+CRC DECODING

A. Polar Encoding

We focus on systematic polar codes [17], whose frozen bit locations are optimized with the method proposed in [20]. Note that this design method does not consider non-uniform bit reliability underlying in high-order QAM and OFDM signaling. Instead of using the conventional SC decoding, we employ the recently proposed list+CRC decoder [18], using CRC-8 given by polynomial 0xD5. Besides frozen bit optimization, there is additional room to design a mapping pattern of the polar-coded bits into the modulation bits across different subcarriers for high-order QAM OFDM transmissions, which have non-uniform reliability, as motivated by the work in [23]. Later, we will discuss the interleaver design to exploit the increased degrees of freedom for bit-interleaved polar-coded OFDM transmissions.

The polar encoding procedure first writes the k data bits into a vector $\mathbf{u} = [u_0, u_1, \dots, u_{N-1}]^T$ of length $N = 2^p$ at a given set of k locations $\mathbb{K} \subset \{0, \dots, N-1\}$, while the remaining $N-k$ locations of \mathbf{u} are frozen to known, fixed values, which in practice can be all zeros. The codeword is then given by $\mathbf{c} = \mathbf{F}^{\otimes p} \mathbf{B} \mathbf{u}$, where the matrix multiplications are carried out over the binary field (i.e., modulo-2 arithmetic), \mathbf{B} denotes an $N \times N$ bit-reversal permutation matrix, and $\mathbf{F}^{\otimes p}$ is the p th Kronecker power of the binary kernel matrix:

$$\mathbf{F} = \begin{bmatrix} 1 & 1 \\ 0 & 1 \end{bmatrix}. \quad (2)$$

The sequential operation of the Kronecker products gives rise to the so-called polarization phenomenon to approach capacity in arbitrary discrete-input memoryless channels [16].

For practical encoding, directly multiplying these matrices can be avoided, since its structure allows an equivalent recursive encoding procedure with a complexity order of $\mathcal{O}(N \log_2 N)$. A particular polar code is fully specified by the data bit locations \mathbb{K} and codeword length $N = 2^p$. For

systematic polar coding [17], the encoding procedure determines the valid codeword \mathbf{c} where the k data bits appear in \mathbf{c} at the locations \mathbb{K} after applying the bit-reversal permutation. A practical systematic encoding procedure [21] is to write the k data bits into a vector \mathbf{u} at the bit-reversal permutation of the locations \mathbb{K} , with the other locations set to zero, and then apply the polar encoding procedure twice, while setting the frozen bit locations (i.e., the locations not in \mathbb{K}) to zero on the intermediate result between the encodings. This procedure for systematic coding transform can be expressed as follows:

$$\mathbf{c} = \mathbf{F}^{\otimes p} \mathbf{B} \phi_{\mathbb{K}}(\mathbf{F}^{\otimes p} \mathbf{B} \mathbf{u}), \quad (3)$$

where $\phi_{\mathbb{K}}(\cdot)$ denotes setting the locations not in \mathbb{K} to zero.

B. Polar Decoding

The original SC decoding proposed in [16] was recently improved by the list+CRC decoder in [18], which incorporates list decoding and an embedded CRC code to improve the performance for short-block polar codes. The SC decoder proceeds sequentially over the bits, from index 0 to $N-1$, where for each index $i \in \{0, 1, \dots, N-1\}$, an estimate \hat{u}_i for bit u_i is made as follows: if $i \notin \mathbb{K}$, then \hat{u}_i is set to the known, fixed value of u_i , otherwise, when $i \in \mathbb{K}$, \hat{u}_i is set to the most likely value for u_i given the channel outputs and assuming that the previous estimates $[\hat{u}_0, \hat{u}_1, \dots, \hat{u}_{i-1}]$ are correct.

The list+CRC decoder proceeds similarly to the SC decoder, except that for each data bit index $i \in \mathbb{K}$, the decoder retains both possible estimates, $\hat{u}_i = 0$ and $\hat{u}_i = 1$, in the subsequent decoding paths. To avoid handling an exponentially increasing number of paths, the list-decoding approach limits the number of paths to a fixed-size list of the most likely partial paths. The list+CRC decoder also employs a CRC code embedded in the data bits, which allows it to select the final decoding as the most likely path with a valid CRC. The combination of list-decoding with the embedded CRC code to reject invalid paths yields significantly improved performance [18].

C. Polar Codes vs. LDPC Codes in AWGN Channels

As reported in [18], the polar codes can outperform LDPC codes that are used in wireless standards even at short block lengths when list+CRC decoding is adopted. Moreover, it was shown in [19] that the polar codes with list+CRC decoding achieve near the Polyanskiy bound of finite-length systems [7]. In [24], the authors verified the advantage of short-length polar codes in AWGN channels even when compared to more recently proposed Pareto-optimal LDPC codes [5], which show the best tradeoff between threshold and decoding complexity by optimizing degree distribution for finite-iteration decoding via extrinsic information transfer (EXIT) trajectory.

For self-consistency, we here re-evaluate the bit-error rate (BER) performance of short-block polar codes to compare with the state-of-the-art LDPC codes [5] in AWGN channels for 4QAM transmission, before moving on to investigating OFDM transmission with high-order QAM in wireless fading channels. Fig. 3(a) compares the BER performance of Pareto-optimal LDPC codes and systematic polar codes. Here, we

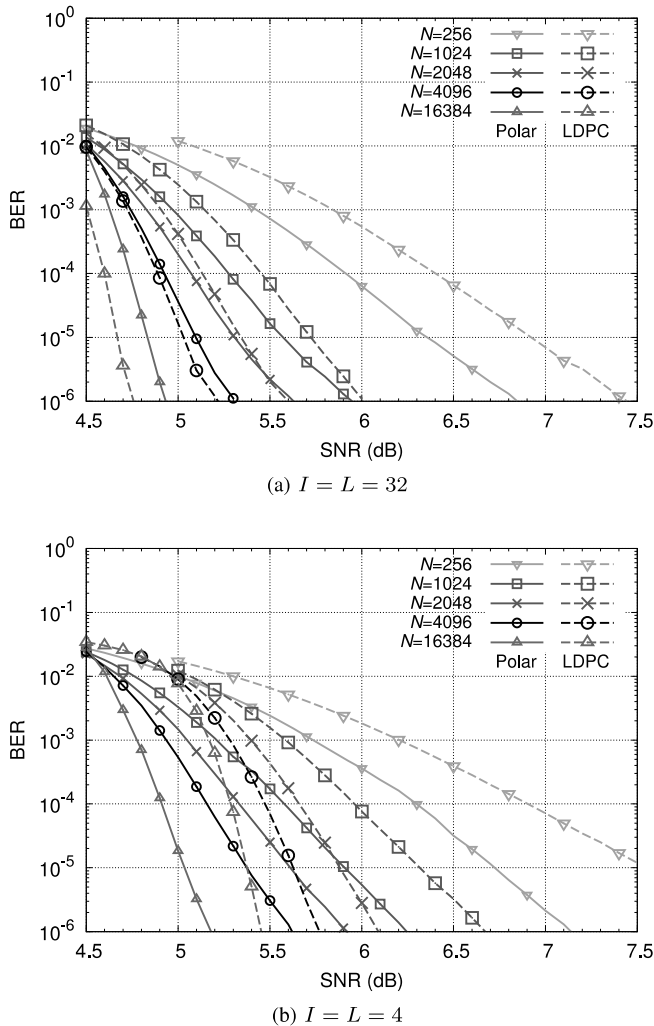


Fig. 3. BER comparison of LDPC codes with I -iteration layered decoding and polar codes with L -list decoding and CRC-8 for various finite-block lengths in AWGN channels.

use $I = 32$ iterations for LDPC layered decoding, and a list size of $L = 32$ for polar decoding (with CRC-8). We consider five block lengths, $N \in \{256, 1024, 2048, 4096, 16384\}$. The code rates for all curves are identical to be $R = 0.8$ (including CRC overheads). As shown in Fig. 3(a), the BER performance can significantly degrade when the block lengths are limited. Hence, the longest possible block lengths that achieve the latency requirements should be used. It is seen in Fig. 3(a) that polar codes with list+CRC decoding can outperform optimized LDPC codes at block lengths shorter than 3000 bits.

The BER performance depends greatly on the decoding complexity, more specifically, the available number of iterations I for LDPC codes and the list size L for polar codes. In Fig. 3(b), we compare BER curves for lower complexity cases of $I = L = 4$. Compared to the case of $I = L = 32$ in Fig. 3(a), most curves shift by approximately 0.5 dB due to the reduced decoder complexity. Nevertheless, the performance loss of polar codes is relatively small compared to that suffered by LDPC codes. Consequently, LDPC codes perform worse

than polar codes for all block lengths we considered. These results suggest that polar codes can be better candidates than LDPC codes for latency- and power-stringent M2M networks.

IV. BIT-INTERLEAVED POLAR-CODED OFDM

A. Interleaver Design for Polar-Coded OFDM

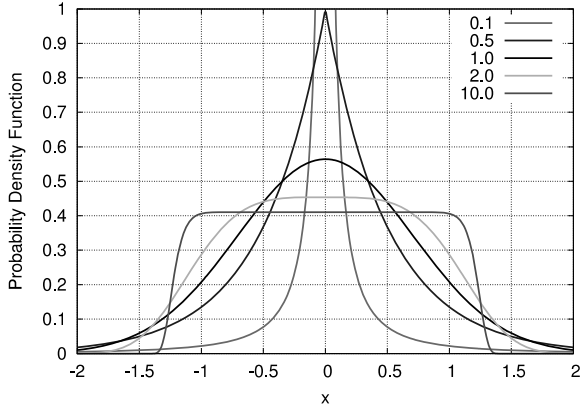
In the previous performance evaluations, we just considered AWGN channels with 4QAM, where all bits have uniform reliability, meaning that BER is not affected by interleaving. In order to reduce the transmission latency, higher-order modulation schemes shall be used for M2M communications. In [23], it was shown that an additional gain can be obtained by designing interleavers to map codewords into high-order modulations. The authors of [23] considered very short mapping patterns up to 16 bits in length, and did not use list-CRC decoding nor OFDM transmissions. In this paper, we consider random, block, and quadratic polynomial permutation (QPP) interleavers [28, 29] to design interleaver parameters, suited for wireless OFDM transmission. The QPP interleaver has been used in wireless standards for turbo coding because of practical advantages: high parallelism factor due to its maximum contention-free property, high flexibility but with a small number of parameters to be optimized, etc.

The n th coded bit is interleaved by QPP as follows:

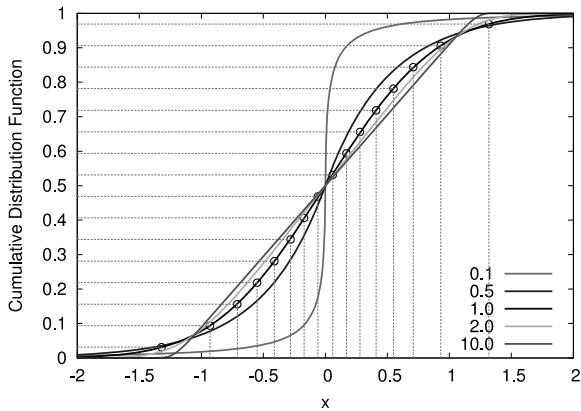
$$\Pi(n) = (f_0 + f_1 n + f_2 n^2) \bmod N, \quad (4)$$

where f_0 , f_1 , and f_2 are interleaver coefficients to be optimized under the constraints that f_1 must be co-prime to N and f_2 must contain all prime factors of N . In [24], we found that the QPP interleaver originally designed for turbo coding is also effective for polar-coded high-order QAMs in AWGN channels. In this paper, we show that an even higher gain is achieved by the QPP interleaver in wireless fading channels. For the QPP interleavers, we search for the best parameters among possible triplets over $f_0 \in \{0, 1, 2, 3\}$, all prime integers no larger than 71 for f_1 , and all power-of-two integers less than N for f_2 . As for the block interleavers, we consider all possible rectangular read-write buffers having the number of columns that is a power-of-two up to N .

As shown in Fig. 2, the instantaneous channel gain may vary over time across different subcarriers. We assume that the channel fluctuation is relatively slow in time and that the transmitter has knowledge of which subcarriers have strong channel gain so that the interleaver can assign more important coded bits into more reliable subcarriers. Based on this assumption, the subcarrier index is sorted in ascending order of its channel gain without loss of generality. In practice, perfect knowledge of channel gain order is not required since the interleaver just exploits the channel selectivity so as not to assign bursts of unreliable subcarriers to important coded bits. Note that shuffling burst channel selectivity is intuitively important since the frozen bit locations, designed by the method in [20], are based on the assumption of uniform channels. Joint optimization of frozen bit location and interleaver is left as a part of future works to further improve the performance.



(a) PDF



(b) CDF

Fig. 4. Super-Gaussian distribution for an order of $\gamma = \{0.1, 0.5, 1, 2, 10\}$. Shaped constellation is determined by equally-spaced CDF points.

B. Super-Gaussian QAM for Geometric Constellation Shaping

Most typically, regular QAM signal constellations are used for communications. However, with such uniformly spaced constellations, codes exhibit a shaping loss which asymptotically approaches 1.53 dB [25]. By using non-uniform spacing [26, 27] for signal constellations, a substantial shaping gain can be achieved. For example, to approach capacity over the AWGN channels, an input distribution that resembles a Gaussian distribution is required. To approximate a Gaussian input distribution, the signals could be spaced more densely around zero.

In this paper, we use geometric shaping to improve regular QAMs, motivated by non-uniform spacing methods in [26, 27]. We extend the work of Gaussian-shaped QAM to super-Gaussian shaping so that we have more degrees of freedom to improve the performance. The m th constellation point ($m \in \{0, 1, \dots, M-1\}$) for shaped M -ary pulse-amplitude modulation (PAM) is chosen such that the corresponding cumulative distribution function (CDF) is equally spaced. For example, since the Gaussian CDF is given by the error function, $F(x) = (1 + \text{erf}(x))/2$, the m th constellation point x_m is chosen such that $F(x_m) = (m+0.5)/M$. Thus, we have

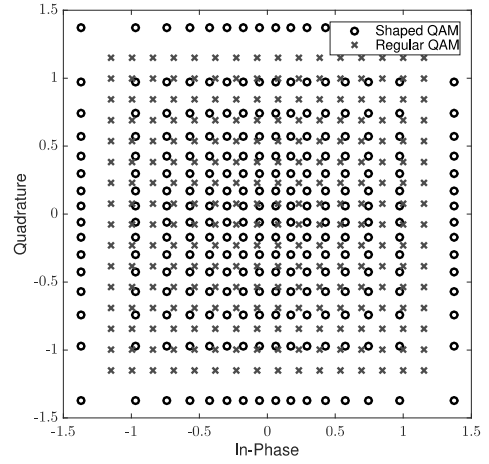


Fig. 5. Super-Gaussian-Shaped 256QAM constellation (Gaussian: $\gamma = 1$, Regular: $\gamma = \infty$).

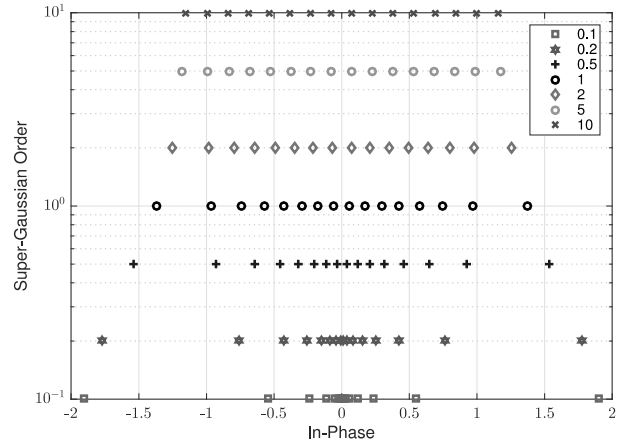


Fig. 6. Super-Gaussian-Shaped 256QAM constellation (in-phase) with different order of γ .

$x_m = \text{erf}^{-1}((2m+1)/M - 1)$. Note that x_m should later be normalized by a constant value to have unit average energy per symbol. This can be generalized to super-Gaussian shaping to provide seamless control of constellation from regular QAM. The probability density function (PDF) and CDF of order- γ super-Gaussian distribution are expressed as follows:

$$f(x) = \frac{1}{2\Gamma(1 + \frac{1}{2\gamma})\sqrt{2\sigma^2}} \exp\left(-\left(\frac{x^2}{2\sigma^2}\right)^\gamma\right), \quad (5)$$

$$F(x) = \begin{cases} \frac{1}{2}\Gamma(\frac{1}{2\gamma}, (\frac{x^2}{2\sigma^2})^\gamma), & x \leq 0, \\ 1 - \frac{1}{2}\Gamma(\frac{1}{2\gamma}, (\frac{x^2}{2\sigma^2})^\gamma), & x > 0, \end{cases} \quad (6)$$

$$\sigma^2 = \frac{3\Gamma(1 + \frac{1}{2\gamma})}{4\Gamma(1 + \frac{3}{2\gamma})}, \quad (7)$$

where $\Gamma(x) = \int_0^\infty t^{x-1} \exp(-t) dt$ and $\Gamma(a, x) = \int_x^\infty t^{a-1} \exp(-t) dt / \Gamma(a)$ are the gamma function and normalized incomplete gamma function, respectively. For $\gamma = 1$, this distribution reduces to a standard Gaussian distribution.

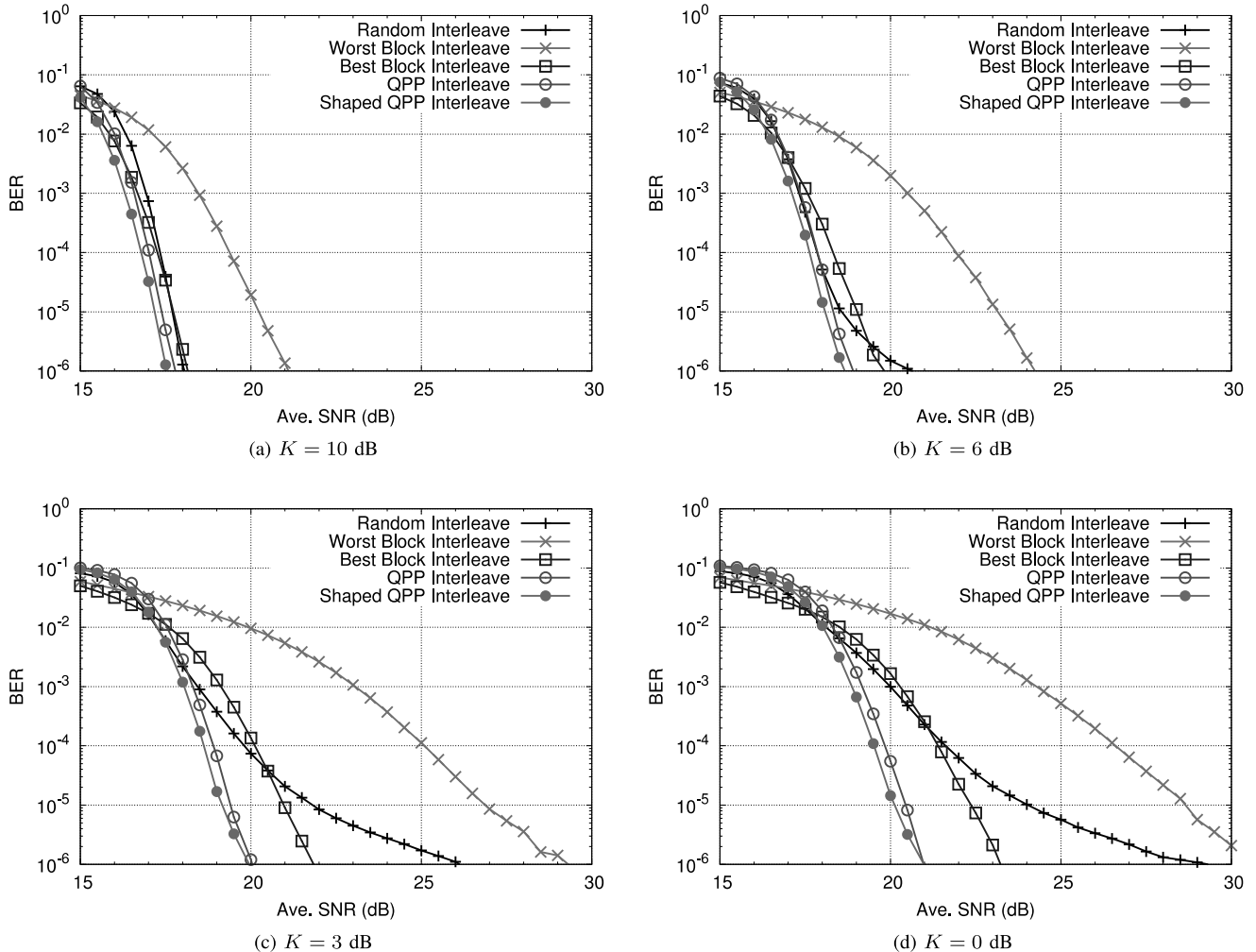


Fig. 7. Bit-interleaved polar-coded 256QAM in Nakagami-Rice fading channels for $N = 1024$, $L = 32$, and CRC-8.

Fig. 4 shows the super-Gaussian PDF and CDF for $\gamma = \{0.1, 0.5, 1, 2, 10\}$. Shaped non-uniform constellation points are selected such that the corresponding CDF point is uniformly distributed, as shown in Fig. 4(b), which illustrates $M = 16$ points, non-uniformly spaced according to the equiprobable Gaussian CDF (i.e., $\gamma = 1$). The non-uniformly spaced M -ary PAM constellations are then used in in-phase and quadrature components to construct shaped M^2 -ary QAM as shown in Fig. 5, which depicts both the regular 256QAM and the shaped 256QAM (with $\gamma = 1$).

By adjusting the order factor γ , we can readily control the Gaussianity of the constellation shaping from uniform shape to impulsive shape. For example, we obtain regular QAM with $\gamma = \infty$. Fig. 6 illustrates the seamless transition of the super-Gaussian 256QAM constellation (in-phase) as a function of the order parameter γ . Note that non-uniform QAM usually performs worse than regular QAM in uncoded BER performance, whereas its mutual information can be improved by mitigating shaping gaps from the Shannon limit in bit-interleaved coded modulation (BICM) systems [30].

C. BER Performance

We now evaluate the benefit of bit-interleaved polar-coded OFDM with the QPP interleaving and shaped QAM in wireless fading channels. Fig. 7 shows the BER improvement that results from optimizing the interleaver for polar codes of length $N = 1024$ for 256QAM in Nakagami-Rice fading channels having different Rician factor $K \in \{10, 6, 4, 0\}$ dB. We assume a code rate of $R = 0.8$. Here, we optimized shaped QAM constellation and interleaver parameters at an average signal-to-noise ratio (SNR) of 17 dB for a Rician factor of $K = 10$ dB. Specifically, we use $\gamma = 2$ for super-Gaussian shaping, 8 columns for the block interleaver, and $(f_0, f_1, f_2) = (2, 7, 16)$ for the QPP interleaver. Note that better parameters can be found at different channel conditions (e.g., Rician factor and SNR), while such parameter adaptation is not carried out in Fig. 7 for simplicity.

We observe that the QPP interleaver with optimized coefficients can perform better than the best block interleaver, and achieve a significant gain that is greater than 0.5 dB. We observe the following results:

- The interleaver needs to be carefully designed for polar-coded OFDM transmissions. The worst block interleaver incurs a considerable penalty of 3–7 dB compared to the best block interleaver.
- The random interleaver suffers a serious diversity loss at high SNR regimes for more scattering wireless environments with smaller Rician factor. This may be because there is higher probability that deeply faded subcarriers are assigned to polar-coded bits in a manner that disrupts the polarization phenomenon of polar coding.
- The QPP interleaver performs best with approximately 2 dB gain against the best block interleaver for dispersive fading channels with $K \leq 3$ dB.
- The performance degradation due to deep fading with smaller Rician factor can be mitigated by polar-coded OFDM employing a well-designed interleaver, effectively exploiting frequency diversity.
- An additional gain up to 0.2 dB can be achieved by the shaped QAM constellation.

V. CONCLUSIONS

For low-latency and highly reliable M2M communications, we investigated a short block-coded modulation based on polar-coded OFDM transmission. We verified that polar codes with list+CRC decoding are promising candidates compared to state-of-the-art LDPC codes for latency-constrained M2M communications with short block and high-order QAM. In addition, we showed that hardware-efficient QPP interleaving with careful parameter selection achieves significant gain greater than 2 dB compared to the conventional random interleaving for polar-coded 256QAM in Nakagami–Rice fading wireless channels. We also introduced non-uniformly spaced QAM for seamless geometric shaping based on super-Gaussian distribution, achieving an additional 0.2 dB gain against the regular QAM.

ACKNOWLEDGMENT

The authors would like to thank Drs. David S. Millar, Kieran Parsons, and Keisuke Kojima for useful discussions.

REFERENCES

- [1] G. Wu, S. Talwar, K. Johansson, N. Himayat, and K. Johnson, “M2M: From mobile to embedded internet,” *IEEE Commun. Magazine*, vol. 49, no. 4, pp. 36–43, 2011.
- [2] S. Kudekar, T. Richardson, and R. Urbanke, “Threshold saturation via spatial coupling: Why convolutional LDPC ensembles perform so well over the BEC,” *IEEE Trans. Inform. Theory*, vol. 57, pp. 803–834, 2011.
- [3] A. Leven and L. Schmalen, “Status and recent advances on forward error correction technologies for lightwave systems,” *J. Lightw. Technol.*, vol. 32, no. 16, pp. 2735–2750, 2014.
- [4] C.-K. Lian, “A partially parallel low-density parity check code decoder with reduced memory for long code-length,” *Ph.D. thesis*, 2007.
- [5] T. Koike-Akino, D. S. Millar, K. Kojima, K. Parsons, Y. Miyata, K. Sugihara, and W. Matsumoto, “Iteration-aware LDPC code design for low-power optical communications,” *J. Lightw. Technol.*, vol. 34, no. 2, pp. 573–581, 2016.
- [6] B. Smith, M. Ardakani, W. Yu, and F. R. Kschischang, “Design of irregular LDPC codes with optimized performance-complexity tradeoff,” *IEEE Trans. Commun.*, vol. 58, no. 2, pp. 489–499, 2010.
- [7] Y. Polyanskiy, H. V. Poor, and S. Verdú, “Channel coding rate in the finite blocklength regime,” *IEEE Trans. Inform. Theory*, vol. 56, no. 5, pp. 2307–2359, 2010.
- [8] D. J. Love and R. W. Heath, “Limited feedback unitary precoding for spatial multiplexing systems,” *IEEE Trans. Inform. Theory*, vol. 51, no. 8, pp. 2967–2976, Aug. 2005.
- [9] R. W. Heath and A. J. Paulraj, “Linear dispersion codes for MIMO systems based on frame theory,” *IEEE Trans. Signal Process.*, vol. 50, no. 10, pp. 2429–2441, Oct. 2002.
- [10] Y. Xin, Z. Wang, and G. B. Giannakis, “Space-time diversity systems based on linear constellation precoding,” *IEEE Trans. Wireless Commun.*, vol. 2, no. 2, pp. 294–304, Mar. 2003.
- [11] M. O. Damen, K. Abed-Meraim, and J. C. Belfiore, “Transmit diversity using rotated constellations with Hadamard transform,” *Adaptive Systems for SP, Com., and Control Conf.*, Lake Louise, Alberta, Canada, Oct. 2000.
- [12] T. Koike-Akino, K. J. Kim, M. Pajovic, and P. V. Orlik, “Universal multi-stage precoding with monomial phase rotation for full-diversity M2M transmission,” *IEEE GLOBECOM*, Dec. 2015.
- [13] R. Annavajjala and P. Orlik, “Achieving near-exponential diversity on uncoded low-dimensional MIMO, multi-user and multi-carrier systems without transmitter CSI,” *IEEE Information Theory and Applications Workshop (ITA)*, pp. 1–11, 2011.
- [14] A. Yellepeddi, K. J. Kim, C. Duan, and P. Orlik, “On probabilistic data association for achieving near-exponential diversity over fading channels,” *IEEE ICC*, pp. 1–6, June 2013.
- [15] M. Pajovic, K. J. Kim, T. Koike-Akino, and P. Orlik, “Modified probabilistic data association algorithms,” *IEEE ICC*, June 2014.
- [16] E. Arkan, “Channel polarization: A method for constructing capacity-achieving codes for symmetric binary-input memoryless channels,” *IEEE Trans. Inform. Theory*, vol. 55, no. 7, pp. 3051–3073, 2009.
- [17] E. Arkan, “Systematic polar coding,” *IEEE Commun. Lett.*, vol. 15, no. 8, pp. 860–862, 2011.
- [18] I. Tal and A. Vardy, “List decoding of polar codes,” *IEEE Trans. Inform. Theory*, vol. 61, no. 5, pp. 2213–2226, 2015.
- [19] B. Li, H. Shen, and D. Tse, “An adaptive successive cancellation list decoder for polar codes with cyclic redundancy check,” *IEEE Commun. Lett.*, vol. 16, no. 12, pp. 2044–2047, 2012.
- [20] I. Tal and A. Vardy, “How to construct polar codes,” *IEEE Trans. Inform. Theory*, vol. 59, no. 10, pp. 6562–6582, 2013.
- [21] G. Sarkis, I. Tal, P. Giard, A. Vardy, C. Thibeault, and W. J. Gross, “Flexible and low-complexity encoding and decoding of systematic polar codes,” *IEEE Trans. Commun.*, vol. 64, no. 7, pp. 2732–2745, 2016.
- [22] M. Seidl, A. Schenk, C. Stierstorfer, and J. B. Huber, “Multilevel polar-coded modulation,” *ISIT*, pp. 1302–1306, 2013.
- [23] D. M. Shin, S. C. Lim, and K. Yang, “Mapping selection and code construction for 2^m -ary polar-coded modulation,” *IEEE Commun. Lett.*, vol. 16, no. 6, pp. 905–908, 2012.
- [24] T. Koike-Akino, Y. Wang, S. C. Draper, K. Sugihara, W. Matsumoto, D. S. Millar, K. Parsons, and K. Kojima, “Bit-interleaved polar-coded modulation for short-block optical transmission,” *submitted to OFC*, Sep. 2017.
- [25] G. D. Forney, Jr. and G. Ungerboeck, “Modulation and coding for linear Gaussian channels,” *IEEE Trans. Inform. Theory*, vol. 44, pp. 2384–2415, Oct. 1998.
- [26] C. Fragouli, R. D. Wesel, D. Sommer, and G. Fettweis, “Turbo codes with non-uniform QAM constellations,” *IEEE ICC*, vol. 1, pp. 70–73, Helsinki, Finland, June 2001.
- [27] F.-W. Sun and H. C. A. van Tilborg, “Approaching capacity by equiprobable signaling on the Gaussian channel,” *IEEE Trans. Inform. Theory*, vol. IT-39, pp. 1714–1716, Sep. 1993.
- [28] O. Y. Takeshita, “On maximum contention-free interleavers and permutation polynomials over integer rings,” *IEEE Trans. Inform. Theory*, vol. 52, no. 3, pp. 1249–1253, 2006.
- [29] J. Sun and O. Y. Takeshita, “Interleavers for turbo codes using permutation polynomials over integer rings,” *IEEE Trans. Inform. Theory*, vol. 51, no. 1, pp. 101–119, Jan. 2005.
- [30] G. Caire, G. Taricco, and E. Biglieri, “Bit-interleaved coded modulation,” *IEEE Trans. Inform. Theory*, vol. 44, pp. 927–945, May 1998.